12. Meerang M, Ritz D, Paliwal S, Garajova Z, Bosshard M, Mailand N, et al. The ubiquitin-selective segregase VCP/p97 orchestrates the response to DNA double-strand breaks. Nat Cell Biol 2011;13: 1376–82.

13. Acs K, Luijsterburg MS, Ackermann L, Salomons FA, Hoppe T, Dantuma NP. The AAA-ATPase VCP/p97 promotes 53BP1 recruitment by removing L3MBTL1 from DNA double-strand breaks. Nat Struct Mol Biol 2011;18:1345–50.

14. Mallette FA, Mattiroli F, Cui G, Young LC, Hendzel MJ, Mer G, et al. RNF8- and RNF168-dependent degradation of KDM4A/JMJD2A triggers 53BP1 recruitment to DNA damage sites. EMBO J 2012;31: 1865–78.

15. Feng L, Chen J. The E3 ligase RNF8 regulates KU80 removal and NHEJ repair. Nat Struct Mol Biol 2012;19:201–6.

16. Luijsterburg MS, Acs K, Ackermann L, Wiegant WW, Bekker-Jensen S, Larsen DH, et al. A new non-catalytic role for ubiquitin ligase RNF8 in unfolding higher-order chromatin structure. EMBO J 2012;31: 2511–27.

17. Kim H, Chen J, Yu X. Ubiquitin-binding protein RAP80 mediates BRCA1-dependent DNA damage response. Science 2007;316: 1202–5.

18. Wang B, Matsuoka S, Ballif BA, Zhang D, Smogorzewska A, Gygi SP, et al. Abraxas and RAP80 form a BRCA1 protein complex required for the DNA damage response. Science 2007;316:1194–8.

19. Sobhian B, Shao G, Lilli DR, Culhane AC, Moreau LA, Xia B, et al. RAP80 targets BRCA1 to specific ubiquitin structures at DNA damage sites. Science 2007;316:1198–202.

20. Sato Y, Yoshikawa A, Mimura H, Yamashita M, Yamagata A, Fukai S. Structural basis for specific recognition of Lys 63-linked polyubiquitin chains by tandem UIMs of RAP80. EMBO J 2009;28:2461–8.

21. Hu Y, Scully R, Sobhian B, Xie A. RAP80-directed tuning of BRCA1 homologous recombination function at ionizing radiation-induced nuclear foci. Genes Dev 2011;25:685–700.

22. Coleman K, Greenberg R. The BRCA1-RAP80 complex regulates DNA repair mechanism utilization by restricting end resection. J Biol Chem 2011;286:13669–80.

23. Nakada S, Tai I, Panier S, Al-Hakim A, Iemura S, Juang YC, et al. Noncanonical inhibition of DNA damage-dependent ubiquitination by OTUB1. Nature 2010;466:941–6.

24. Bouwman P, Aly A, Escandell JM, Pieterse M, Bartkova J, van der Gulden H, et al. 53BP1 loss rescues BRCA1 deficiency and is associated with triple-negative and BRCA-mutated breast cancers. Nat Struct Mol Biol 2010;17:688–95.

25. Bunting SF, Callén E, Wong N, Chen HT, Polato F, Gunn A, et al. 53BP1 inhibits homologous recombination in Brca1-deficient cells by blocking resection of DNA breaks. Cell 2010;141:243–54.

26. Pierce J, Johnson RD, Thompson LH, Jasin M. XRCC3 promotes homology-directed repair of DNA damage in mammalian cells. Genes Dev 1999;13:2633–8.

27. Shiomi N, Mori M, Tsuji H, Imai T, Inoue H, Tateishi S, et al. Human RAD18 is involved in S phase-specific single-strand break repair without PCNA monoubiquitination. Nucleic Acids Res 2007;35:e9.

28. Martin S, Ouchi T. BRCA1 phosphorylation regulates caspase-3 activation in UV-induced apoptosis. Cancer Res 2005;65:10657–62.

29. Ganesan S, Silver DP, Greenberg RA, Avni D, Drapkin R, Miron A, et al. BRCA1 supports XIST RNA concentration on the inactive X chromosome. Cell 2002;111:393–405.

30. Stiff T. ATM and DNA-PK function redundantly to phosphorylate H2AX after exposure to ionizing radiation. Cancer Res 2004;64:2390–6.

31. Sakasai R, Tibbetts R. RNF8-dependent and RNF8-independent regulation of 53BP1 in response to DNA damage. J Biol Chem 2008; 283:13549–55.

32. Murakawa Y, Sonoda E, Barber LJ, Zeng W, Yokomori K, Kimura H, et al. Inhibitors of the proteasome suppress homologous DNA recombination in mammalian cells. Cancer Res 2007;67:8536–43.

33. Huang J, Huen MS, Kim H, Leung CC, Glover JN, Yu X, et al. RAD18 transmits DNA damage signalling to elicit homologous recombination repair. Nat Cell Biol 2009;11:592–603.

34. Schlegel BP, Jodelka FM, Nunez R. BRCA1 promotes induction of ssDNA by ionizing radiation. Cancer Res 2006;66:5181–9.

35. Stewart GS, Stankovic T, Byrd PJ, Wechsler T, Miller ES, Huissoon A, et al. RIDDLE immunodeficiency syndrome is linked to defects in 53BP1-mediated DNA damage signaling. Proc Nat Acad Sci U S A 2007;104:16910–5.

36. Nahas S, Gatti RA. DNA double strand break repair defects, primary immunodeficiency disorders, and 'radiosensitivity'. Curr Opin Allergy Clin Immunol 2009;9:510–6.

37. Santos MA, Huen MS, Jankovic M, Chen HT, López-Contreras AJ, Klein IA, et al. Class switching and meiotic defects in mice lacking the E3 ubiquitin ligase RNF8. J Exp Med 2010;207:973–81.

38. Li L, Halaby MJ, Hakem A, Cardoso R, El Ghamrasni S, Harding S, et al. Rnf8 deficiency impairs class switch recombination, spermatogenesis, and genomic integrity and predisposes for cancer. J Exp Med 2010;207:983–97.

39. Nakada S. Abnormalities in DNA double-strand break response beyond primary immunodeficiency. Int J Hematol 2011;93:425–33.

40. Galanty Y, Belotserkovskaya R, Coates J, Jackson SP. RNF4, a SUMO-targeted ubiquitin E3 ligase, promotes DNA double-strand break repair. Genes Dev 2012;26:1179–95.

41. Morris JR, Solomon E. BRCA1: BARD1 induces the formation of conjugated ubiquitin structures, dependent on K6 of ubiquitin, in cells during DNA replication and repair. Hum Mol Genet 2004;13:807–17.

42. Zhu Q, Pao GM, Huynh AM, Suh H, Tonnu N, Nederlof PM, et al. BRCA1 tumour suppression occurs via heterochromatin-mediated silencing. Nature 2011;477:179–84.

43. Reid LJ, Shakya R, Modi AP, Lokshin M, Cheng JT, Jasin M, et al. E3 ligase activity of BRCA1 is not essential for mammalian cell viability or homology-directed repair of double-strand DNA breaks. Proc Natl Acad Sci U S A 2008;105:20876–81.

44. Drost R, Bouwman P, Rottenberg S, Boon U, Schut E, Klarenbeek S, et al. BRCA1 RING function is essential for tumor suppression but dispensable for therapy resistance. Cancer Cell 2011;20:797–809.

45. Shakya R, Reid LJ, Reczek CR, Cole F, Egli D, Lin CS, et al. BRCA1 tumor suppression depends on BRCT phosphoprotein binding, but not its E3 ligase activity. Science 2011;334:525–8.

46. Sy SM, Jiang J, Dong SS, Lok GT, Wu J, Cai H, et al. Critical roles of ring finger protein RNF8 in replication stress responses. J Biol Chem 2011;286:22355–61.
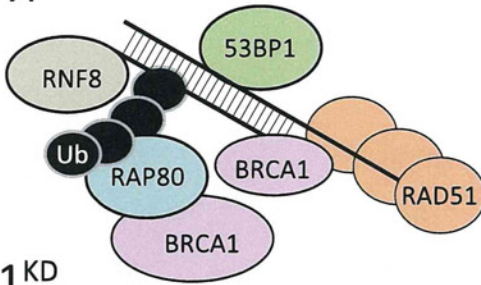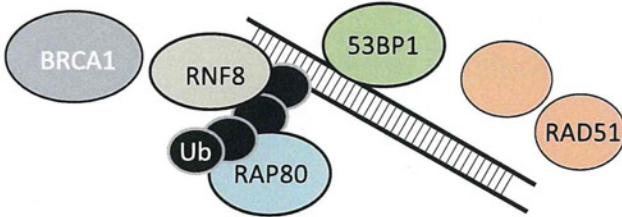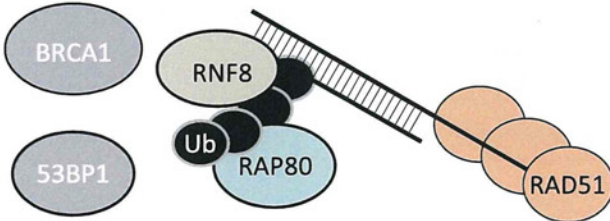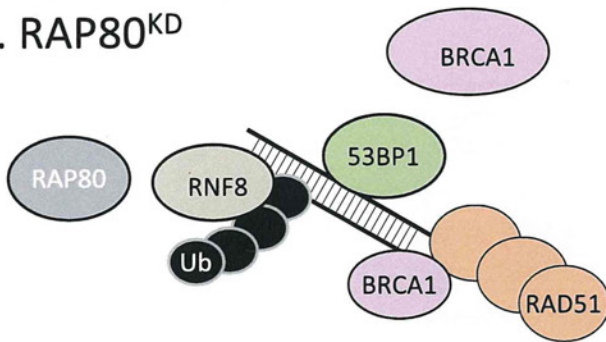
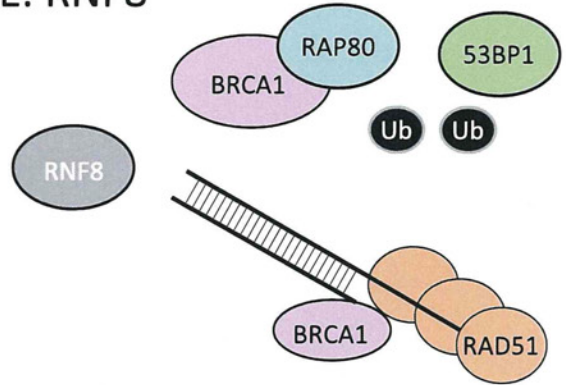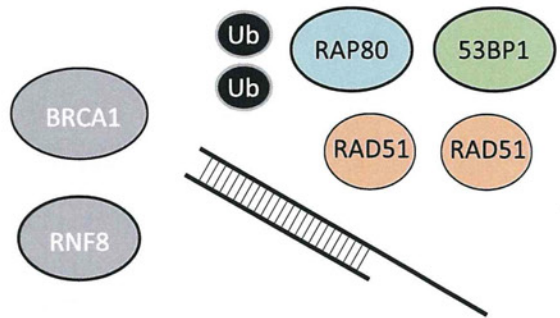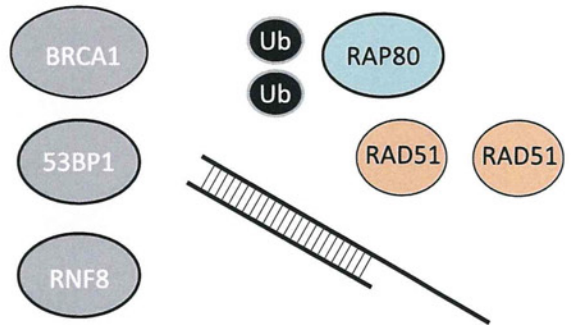**Supplementary Figure 1. A schematic of the assembly of DNA damage response-related proteins at DSB sites. A,** Ubiquitin chain, RAP80, BRCA1, 53BP1 and RAD51 assemble at DSB sites in normal cells. **B,** The ubiquitin chain, RAP80 and 53BP1 but not RAD51 assemble at DSB sites in BRCA1-depleted cells. **C,** The ubiquitin chain, RAP80 and RAD51 assemble at DSB sites in BRCA1/53BP1-depleted cells. **D,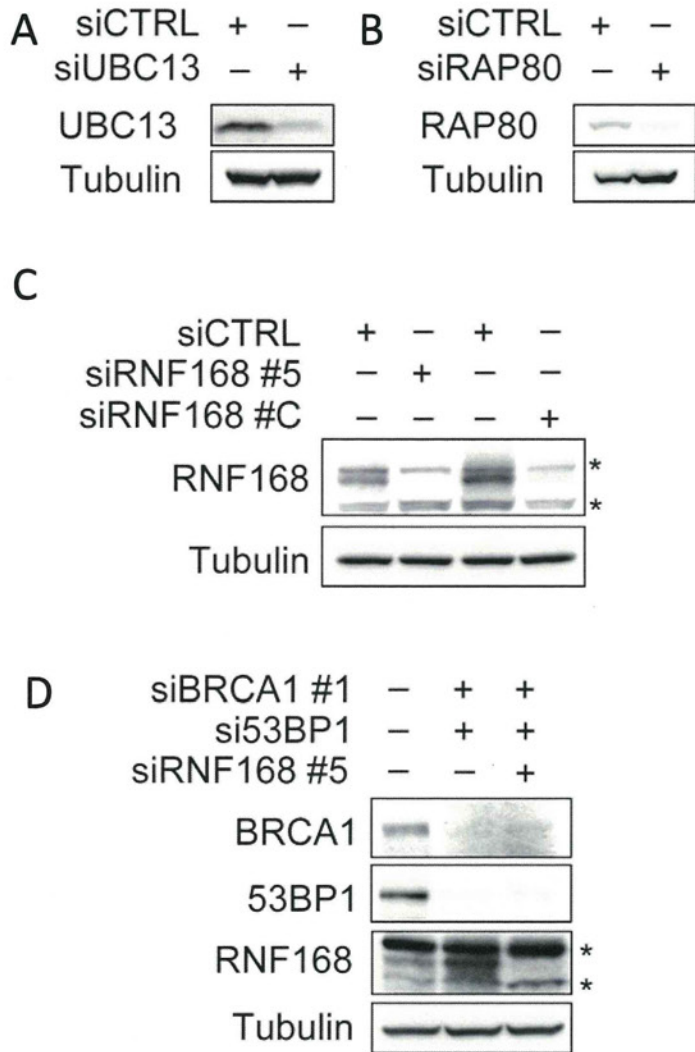** The ubiquitin chain, a small subset of BRCA1 protein, 53BP1 and RAD51 assemble at DSB sites in RAP80-depleted cells. **E,** A small subset of BRCA1 protein and RAD51 but not the ubiquitin chain or 53BP1 assemble at DSB sites in RNF8-depleted cells. **F, G,** The ubiquitin chain, RAD51, BRCA1 and 53BP1 do not assemble at DSB sites in RNF8/BRCA1-depleted cells or RNF8/BRCA1 /53BP1-depleted cells.

A siCTRL + −   **B** siCTRL + −
    siUBC13 − +   siRAP80 − +

UBC13   RAP80

Tubulin   Tubulin

C
siCTRL   + − + −
siRNF168 #5   − + − −
siRNF168 #C   − − − +

RNF168   *
                                *

Tubulin

D
siBRCA1 #1   − + +
si53BP1   − + +
siRNF168 #5   − − +

BRCA1

53BP1

RNF168   *
                        *

Tubulin

Supplementary Figure 2. The effective knockdown of UBC13, RAP80 or RNF168 was confirmed using western blotting. U2OS **(A)**, HeLa **(B)** or HCT116 **(C, D)** cells transfected with indicated siRNAs were subjected to western blotting for the indicated proteins. *non-specific bands.
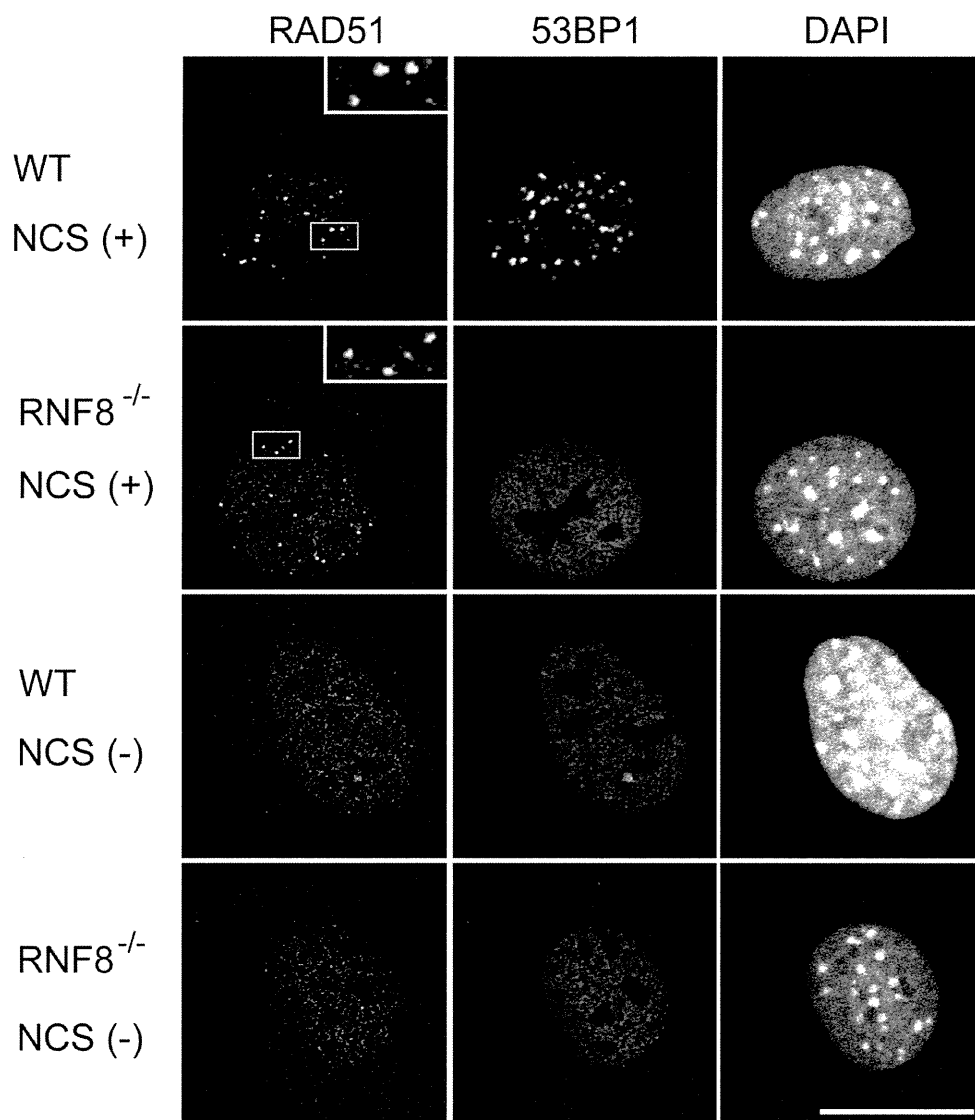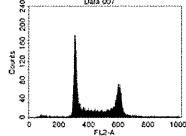
Supplementary Figure 3. RAD51 assembles at DSB sites in RNF8$^{-/-}$ MEFs. WT and RNF8$^{-/-}$ MEFs were treated with 5 ng/ml NCS for 10 min and then subjected to immunofluorescence with the indicated antibodies at 5 hr post-NCS treatment. The area enclosed by each rectangle is magnified. Scale bar, 10 μm
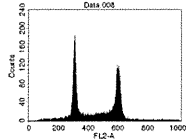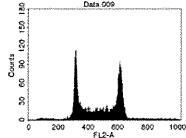
A
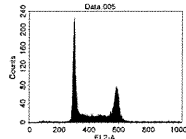
siCTRL
S-G2 phase: 47.4%
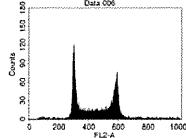
siBRCA1 #1
S-G2 phase: 56.0%

siRNF8 #D
S-G2 phase: 51.0%

siRNF8 #2
S-G2 phase: 54.7%

siBRCA1 #1 + siRNF8 #D
S-G2 phase: 60.2%
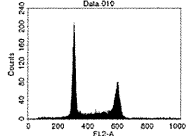
siBRCA1 #1 + siRNF8 #2
S-G2 phase: 47.9%

B
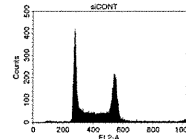
siCTRL
S-G2 phase: 54.2%
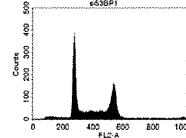
si53BP1
S-G2 phase: 47.8%
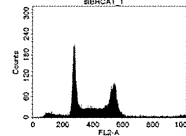
siBRCA1 #1
S-G2 phase: 50.0%
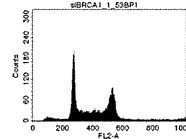
siBRCA1 #1 + si53BP1
S-G2 phase: 50.6%
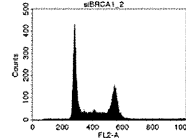
siBRCA1 #2
S-G2 phase: 47.4%
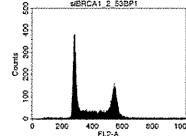
siBRCA1 #2 + si53BP1
S-G2 phase: 49.5%

C
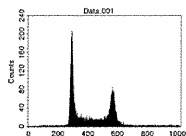
siCTRL
S-G2 phase: 49.3%
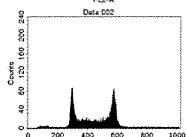
siRNF8 #D + siBRCA1 #1 + si53BP1
S-G2 phase: 61.8%
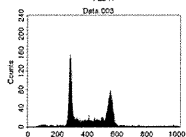
siRNF8 #2 + siBRCA1 #1 + si53BP1
S-G2 phase: 53.3%
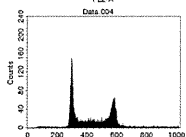
siBRCA1#1 + si53BP1
S-G2 phase: 51.5%

Supplementary Figure 4. Cell cycle analysis. HCT116 cells transfected with various combinations of non-targeting, BRCA1-specific, 53BP1-specific and RNF8-specific siRNAs were fixed, stained with PI and then subjected to cell-cycle analysis using flow cytometry. BRCA1 and RNF8 were simultaneously depleted **(A)**. BRCA1 and 53BP1 were simultaneously depleted **(B)**. RNF8, BRCA1 and 53BP1 were simultaneously depleted **(C)**.
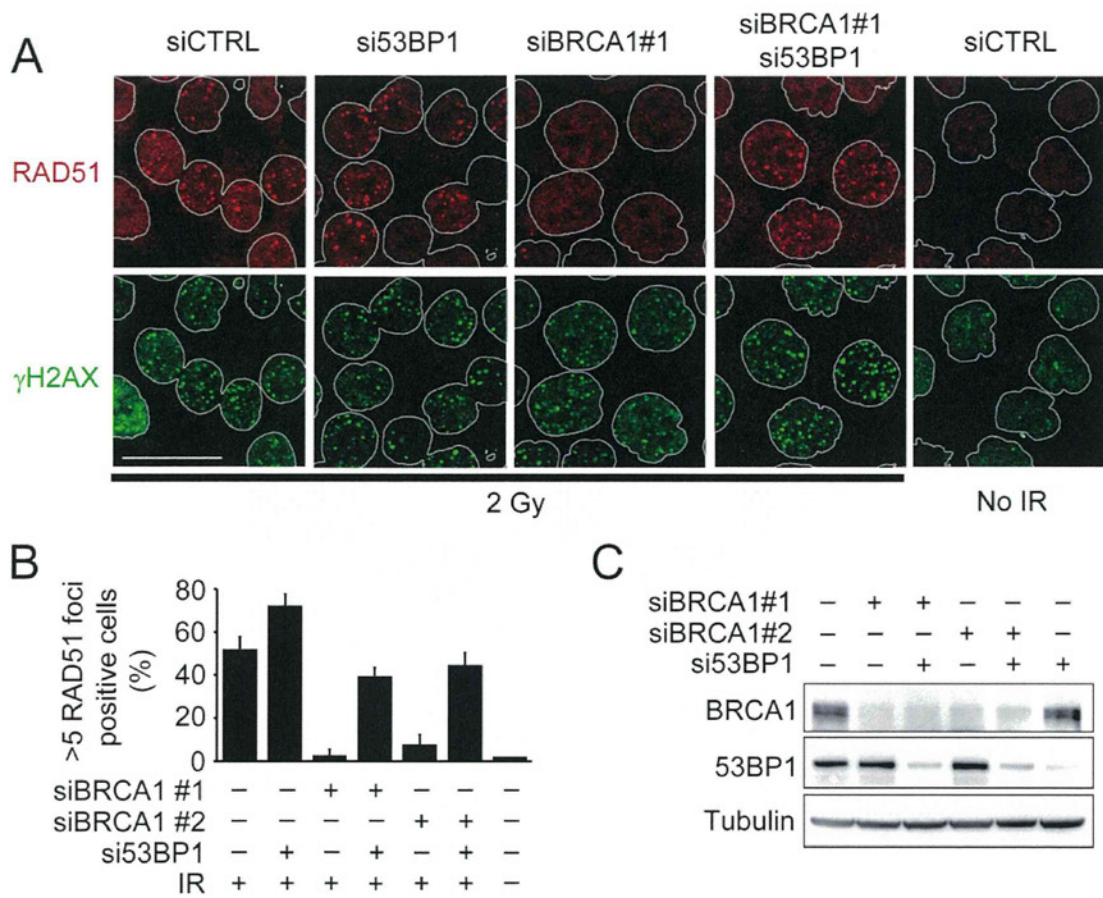
Supplementary Figure 5. Depletion of 53BP1 rescues RAD51 assembly at DSB sites in BRCA1-depleted human cells. A-B, HCT116 cells transfected with the indicated siRNAs were irradiated with 2 Gy and analyzed for RAD51 and gH2AX immunofluorescence at 6 h post-ionizing radiation. Representative images. Scale bar, 25 μm **(A)**. The quantification of cells with >5 RAD51 foci (mean ± s.d., *N* = 3) **(B)**. **C**, HCT116 cells transfected with the indicated siRNAs were subjected to western blotting for the indicated proteins.
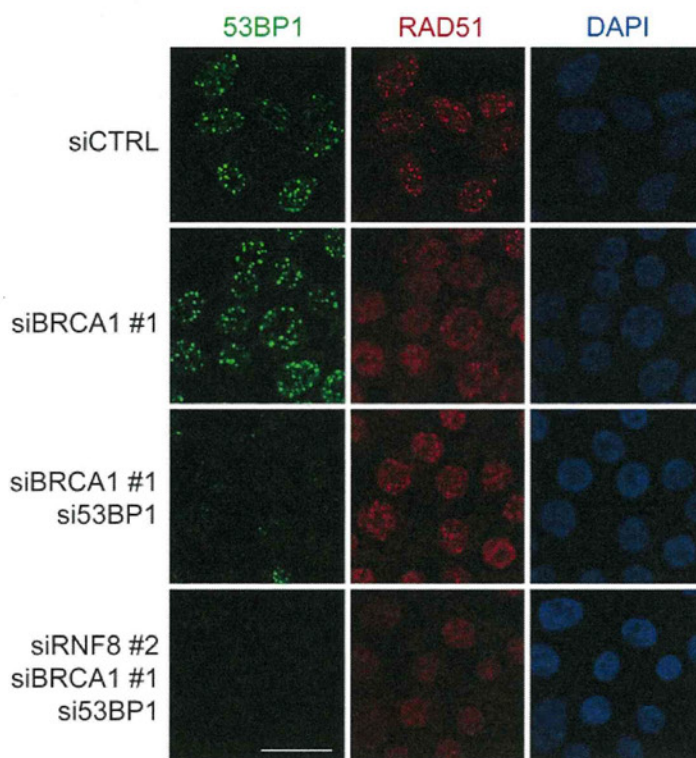
Supplementary Figure 6. RNF8 suppresses RAD51 assembly in BRCA1/53BP1-depleted 293T cells. 293T cells transfected with the indicated siRNAs were irradiated with 2 Gy and analyzed for RAD51 and 53BP1 immunofluorescence at 4 h post-ionizing radiation. Representative images. Scale bar, 25 μm
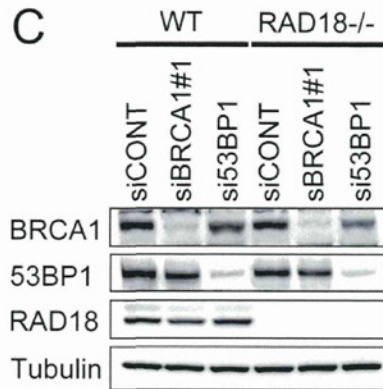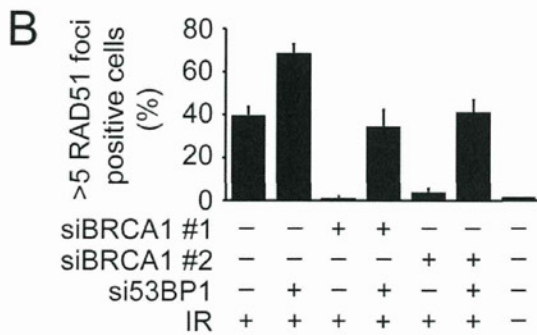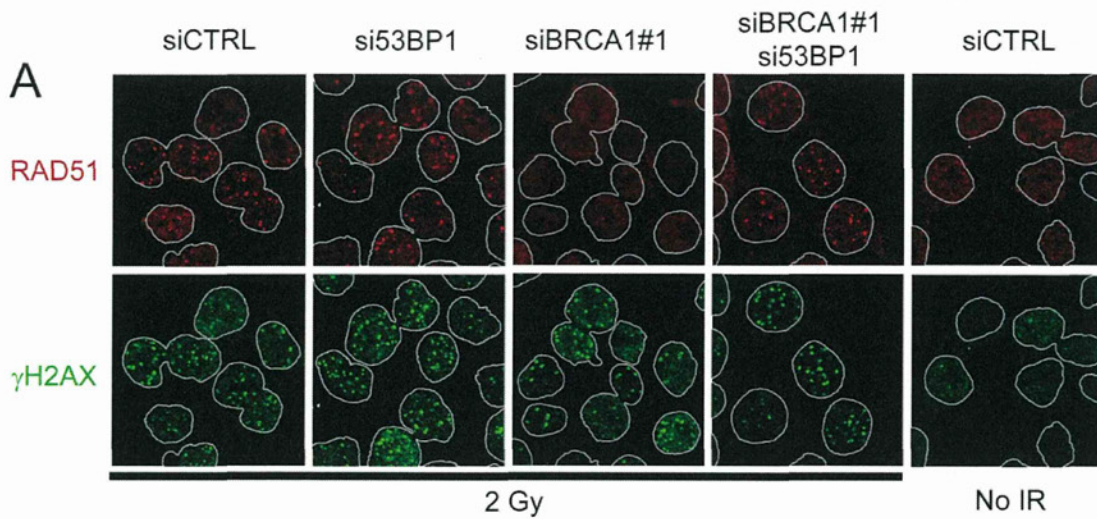
Supplementary Figure 7. RAD18 is not required for RAD51 assembly at DSB sites in the absence of BRCA1 and 53BP1. A-B, *RAD18*$^{-/-}$ HCT116 cells transfected with the indicated siRNAs were irradiated with 2 Gy and analyzed for RAD51 and gH2AX immunofluorescence at 6 h post-ionizing radiation. Representative images. Scale bar, 25 μm **(A)**. The quantification of cells with >5 RAD51 foci (mean ± s.d., *N* = 3) **(B). C**. HCT116 (WT) and *RAD18*$^{-/-}$ HCT116 cells transfected with indicated siRNAs were subjected to western blotting for the indicated proteins. The expression level of BRCA1 and 53BP1 was similar in and *RAD18*$^{-/-}$ HCT116 cells

PRECLINICAL STUDY

Estrogen receptor-α directly regulates sensitivity to paclitaxel in neoadjuvant chemotherapy for breast cancer

Emi Tokuda · Yuko Seino · Atsushi Arakawa ·
Mitsue Saito · Fujio Kasumi · Shin-ichi Hayashi ·
Yuri Yamaguchi

Abstract Neoadjuvant chemotherapy (NAC) has become the standard treatment for advanced breast cancer. Several prognostic markers, including estrogen receptor-α (ERα), are used to predict the response to NAC. However, the molecular significance of ERα expression in the efficacy of chemotherapy is not yet fully understood. To examine this issue, we first evaluated ERα transcriptional activity in breast cancer cells derived from pre-NAC specimens using estrogen response element–green fluorescent protein (ERE–GFP) as a reporter gene, and found that, in the cases for which ERα activities determined by GFP expression were not detected or low, pCR (pathological complete response) could be achieved even though ERα protein was expressed. Next, we examined the effects of alterations in ERα expression levels on sensitivity to paclitaxel, a key drug in NAC, by stable expression of ERα in ER-negative SKBR3 cells and by siRNA-mediated down-regulation of ERα in ER-positive MCF-7 cells, and showed that ERα expression and sensitivity to paclitaxel showed an inverse correlation. We also established paclitaxel-resistant MCF-7 cell clones and found that they have higher estrogen-induced ER activity than parent cells. Paclitaxel is a microtubule-stabilizing agent, while HDAC6 (histone deacetylase 6), which we previously identified as an estrogen-regulated gene, enhances cell motility by desta-bilizing microtubules via deacetylation of α-tubulin. Finally, we demonstrate herein that ERα knockdown in MCF-7 cells prevents deacetylation of α-tubulin, thereby increasing sensitivity to paclitaxel. Taken together, these results suggest that ERα expression directly regulates sensitivity to paclitaxel in NAC for breast cancer via the effect on microtubule stability.

Introduction

Several recent trials have suggested that adjuvant chemotherapy is less effective in patients with estrogen receptor (ER)-positive breast cancers [1–3]. For example, the Cancer and Leukemia Group B9344 trial evaluated the efficacy of anthracycline regimens with or without paclitaxel in adjuvant therapy and found them to be effective in 24% of ER-negative but only 11% of ER-positive patients [2]. Neoadjuvant chemotherapy (NAC) trials of anthracyclines combined with paclitaxel also showed higher pathological complete response (pCR) rates in ER-negative than in ER-positive patients [4, 5].

Recently, NAC has become the standard treatment for advanced breast cancer. NAC has numerous advantages, including down-staging of an inoperable cancer to an operable one, the availability of breast conservation for

E. Tokuda · M. Saito · F. Kasumi
Department of Breast and Endocrine Surgery, Graduate School of Medicine, Juntendo University, Tokyo, Japan

E. Tokuda · Y. Seino · Y. Yamaguchi (✉)
Research Institute for Clinical Oncology, Saitama Cancer Center, 818 Komuro, Ina-machi, Saitama-ken 362-0806, Japan
e-mail: yamaguchi@cancer-c.pref.saitama.jp

Y. Seino · S. Hayashi
Center for Regulatory Epigenome and Diseases, Department of Molecular and Functional Dynamics, Graduate School of Medicine, Tohoku University, Sendai, Japan

A. Arakawa
Department of Human Pathology, Juntendo University Hospital, Tokyo, Japan

patients who would otherwise undergo a mastectomy, and the use of pathological response data as a surrogate marker for long-term clinical outcome [6–9]. Another advantage of NAC is that responsiveness to the particular chemotherapy regimen can be assessed, possibly allowing for individualized therapy [10].

Taxanes are potent antimicrotubule agents, which act by inducing tubulin polymerization and promoting the formation of unusually stable microtubules, thereby inhibiting the normal dynamic reorganization of the microtubular network required for mitosis and cell proliferation [11]. Paclitaxel was the first marketed taxane drug affecting the integrity of microtubules. In recent studies, paclitaxel-based combination chemotherapy has resulted in an improved pCR rate as compared with single-agent taxane treatments [12, 13]. Several prognostic markers of NAC, including ERα, are used to predict responses to paclitaxel. For example, patients with ER-positive breast cancers reportedly gain little benefit from the administration of paclitaxel [14, 15]. However, the molecular mechanisms underlying the role of ERα in the efficacy of paclitaxel are not yet fully understood.

We have studied the roles of ERα expression and estrogen-regulated genes as predictors of the efficacy of systemic therapy for ER-positive breast cancer. In our previous studies, we identified histone deacetylase 6 (HDAC6) as an estrogen-regulated gene using cDNA microarray analysis in the ER-positive breast cancer cell line MCF-7 [16]. In the setting of breast cancer, high HDAC6 expression was also detected [17]. HDAC6 was originally cloned as a member of the histone deacetylase family, is expressed in several tissues, and functions as a deacetylase for tubulin [18]. Furthermore, tubulin is an important component of the microtubule network that regulates cell motility, which appears to be enhanced by HDAC6. Accordingly, we hypothesized that microtubule conformation is the common target for estrogen signals and paclitaxel.

To our knowledge, this is the first study designed to clarify the significance of ERα in tumor sensitivity to paclitaxel, via estrogen-induced deacetylation of tubulin mediated by HDAC6.

Materials and methods

Cell culture and reagents

The human breast cancer cell lines MCF-7 and SKBR3 were cultured in RPMI 1640 (Sigma-Aldrich, MO) supplemented with 10% fetal calf serum (FCS; Tissue Culture Biologicals, CA) and antibiotics. All cells were incubated at 37°C under 5% CO_2 in air.

MCF-7–E10 cells (E10 cells) were established from the MCF-7 by introducing a plasmid carrying the ERE (estrogen responsive element) fused with tk-GFP (green fluorescent protein) gene, as described previously [19, 20]. E2 (17β-estradiol) was purchased from Sigma-Aldrich. Paclitaxel was provided by Bristol-Myers Squibb (NY, USA). The paclitaxel-resistant MCF-7–E10 clones (PAC-1–PAC-3) were developed by increasing the paclitaxel dose, stepwise, from 2 to 10 nM, over 2 months.

Assays of cell growth

The cells (5×10^4/well) were seeded in 24-well plates and cultured. After 48 h, the cells were treated with paclitaxel (0–30 nmol/l) for 3 days. Cell numbers were determined using a cell counter (Coulter Counter ZBI; Beckman Coulter, CA) and presented as percentages relative to those of control cells cultured in the absence of anticancer agents. IC50 values (drug dosages producing 50% inhibition of cell growth) were determined from growth inhibition curves.

Knockdown of ERα by siRNA transfection in MCF-7 cells

Cells (1×10^5/well) were cultured in RPMI medium for 24 h. In accordance with the manufacturer's instructions, 10 nmol/l small interfering RNA [ESR1-7255 (Sigma; si-1) and ESR1-7257 (Sigma; si-2) siRNAs for knockdown of ERα] or scramble siRNA (SC-37007, Santa Cruz Biotechnology, CA) was mixed with siLentFect Lipid Reagent (Bio-Rad, CA) in serum-free RPMI. After 20 min, solutions were added to the cells. To investigate the effects of ERα knockdown, cells were harvested and ERα expression was determined by western blotting using anti-ERα antibody (sc-7207, 1/200, Santa Cruz).

Establishment of SKBR3 cells expressing ERα

ER-negative and HER2-positive SKBR3 cells were transfected with an expression plasmid vector for ERα using Trans IT-LT1 (Mirus Bio, WI) following the manufacturer's specifications, and were subjected to selection in growth medium containing geneticin (Sigma). We confirmed ERα expression employing real-time RT-PCR. We use the term SKBR3-cont to indicate cells transfected with control vector, while SK-ERpos cells were transfected with ERα.

Western blot analysis

Cell lysates were prepared using Lysis-M Reagent (Roche Diagnostics, Germany) according to the manufacturer's

instructions. Total proteins (40 µg) were run on SDS-PAGE using 10% acrylamide gels (SuperSep™ace; Wako, Japan) and proteins were transferred onto a PVDF membrane (Bio-Rad). After blocking the membrane with 10% dry milk for 1 h, blots were probed with an antibody to ERα (sc-7207), α-tubulin (sc-5546, 1/200, Santa Cruz), β-tubulin (#2146, 1/1000, Cell Signaling Technology, MA), or acetylated α-tubulin (6-11B-1, 1/2000, Sigma-Aldrich) in 0.05% Tween-20 in TBS (TTBS) at 4°C overnight. Secondary antibodies used at room temperature for 1 h were as follows: goat anti-rabbit IgG (Immun-Star Goat Anti-Rabbit-AP, 1/3000; Bio-Rad) for ERα, α-tubulin and β-tubulin, goat anti-mouse IgG (Immun-Star Goat Anti Mouse-AP, 1/3000; Bio-Rad) for anti-acetylated α-tubulin. An Immun-Star™ chemiluminescent Protein Detection System (Bio-Rad) was used to detect the secondary probes. The image was captured on an LAS-4000 with accompanying Image Reader (Fujifilm, Tokyo Japan). Protein expression was analyzed using Multi Gauge v3.2 software (Fujifilm).

Real-time quantitative RT-PCR

RNA was extracted from whole cells using Isogen (Nippon Gene, Tokyo, Japan) according to the manufacturer's instructions. cDNAs were synthesized from 1 µg of total RNA using a TaKaRa RNA PCR Kit Ver.3.0 (Takara Bio, Shiga, Japan). Real-time quantitative RT-PCR was performed using the LightCycler 2.0 (Roche Diagnostics) with LightCycler FastStart DNA Masterplus SYBR Green 1 kit (Roche Diagnostics). Target gene expression was normalized to the glyceraldehyde-3-phosphate dehydrogenase (GAPDH) expression level. For PCR, the following ERα primer sequences were used: forward, 5′-CTCCCACATC AGGCACAT-3′; reverse, 5′-CTCCAGCAGCAGGCTA TA-3′. The HDAC6 primers were as follows: forward, 5′-GTCTACTGTGGTCGTTACATC-3′; reverse, 5′-GGC CTGACAGTAACAC-3′.

Patients received NAC at Juntendo University Hospital

All patients who received NAC had tumors over 3 cm in diameter and/or positive axillary nodes, but no distant metastasis prior to NAC. Determinations of invasive cancer, hormone receptor status, and HER2 status were based on pre-NAC core needle biopsy results.

The patients received four cycles of fluorouracil (500 mg/m^2), epirubicin (75 or 100 mg/m^2), and cyclophosphamide (500 mg/m^2) (FEC), followed by taxanes, namely, 12 weekly cycles of paclitaxel (80 mg/m^2) or docetaxel (150 mg/m^2) every 3 weeks for four cycles. Sonography plus MRI was carried out at diagnosis, then again prior to the administration of taxanes, and before

surgery. A clinical complete response (cCR) was disappearance of the tumor on these images. A clinical partial response (cPR) was more than 30% shrinkage of the tumor with NAC, and clinical progressive disease (cPD) was a more 20% increase in the tumor. Any response other than these was categorized as clinical stable disease (cSD). A pathological CR (pCR) involved no evidence of intraductal components or metastatic lesions.

We first analyzed 190 patients with advanced breast cancer who received NAC at the Breast Center of Juntendo University Hospital (Tokyo, Japan) between July 2006 and January 2008. To assess the relationships between ER activity in breast cancer cells and the clinical response to NAC, we analyzed 31 breast cancer tissues, obtained by core needle biopsy and/or surgical resection at Juntendo University Hospital from June 2009 to March 2010. All tumor specimens were obtained after informed consent from patients. The Juntendo University Hospital Ethics Committee approved this study.

Immunohistochemistry (IHC)

ER status was determined using IHC methods. Slides were stained and evaluated using the Ventana I-VIEW Breast Panel (Roche). Immunoreactivity greater than 10% was considered to indicate receptor-positive status. HER2 protein status, as assessed using the Herceptest (Ventana, Switzerland), was scored on a scale of 0 to 3+ according to the Dako scoring system. HER2/neu-positive status was defined as HER2 protein 3+ or 2+ and a fluorescence in situ hybridization (FISH) ratio of more than 2.2.

Assay of ERE activity in primary tumor cells (adenovirus ERE–GFP method)

To assess ERE activation in primary tumor cells, we used Ad-ERE-tk-GFP [20, 21]. Cancer tissue specimens were minced to ∼1 mm^3 after rinsing with PBS and digested with collagenase solution for 20–30 min at 37°C. The cells, including tumor cells, were washed several times with PBS, and incubated in 24-well plates using 400 µl of phenol-red-free RPMI 1640 supplemented with 10% heat- and charcoal-treated fetal calf serum (DCC-FCS). The cells were then infected, either immediately or 1 day later, with 2 × 10^9 PFU (plaque-forming units) (in 293A cells) of Ad-ERE-tk-GFP, and incubated for 3 days. GFP-expressing cells were counted by fluorescence microscopy after incubation. To examine the infectivity of the adenovirus in primary tumor cells, the cells were infected with 2 × 10^9 PFU of Ad-CMV-DsRed, and at least 95% of cells were confirmed to be infected [21]. When more than 10% of cancer cells expressed GFP, the specimen was considered to have high ER transcriptional activity.

Detection of ER activity in MCF-7 and sublines

To quantify the ER activities of MCF-7–E10 cells and PAC-1–PAC-3 cells in terms of the intensity of GFP expression, we previously developed an automated image analysis system for GFP expression in collaboration with Olympus Life Science Company (Tokyo, Japan) [22]. Using this system, estrogen-induced ER activation was analyzed.

Statistical analysis

Statistical analyses were performed using the Stat Flex version software program (Artech Co., Ltd., Osaka, Japan). In comparisons among three or more groups, ANOVA, two-sample t tests, and Fisher's exact test were used to assess the statistical significance of differences. Data are expressed as means ± SD $P < 0.05$ was considered statistically significant.

Results

Clinical response to taxanes in NAC

First, we studied the relationship between ER expression and clinical response to taxanes in 190 breast cancer patients receiving NAC. As shown in Table 1, 6.8% of the 190 patients showed cCR (clinical complete response) by taxanes. ER-negative patients achieved a higher cCR rate than ER-positive patients (12.5 vs. 4.0%, $P = 0.028$), while no significant difference in cCR rate was observed for HER2 expression ($P = 0.498$). ER-negative patients also tended to have a higher cCR plus cPR (clinical partial response) rate than ER-positive patients (57.9 vs. 42.9%, $P = 0.051$). These results suggest ER-negative breast cancers to be more sensitive to taxanes than ER-positive cancers.

Table 1 Clinical complete response to taxanes in NAC-treated patients

Characteristic	cCR rate of patients	
	No./total (%)	
ER		
Positive ($n = 126$)	5/126 (4.0)	$P = 0.028*$
Negative ($n = 64$)	8/64 (12.5)	
HER2		
Positive ($n = 71$)	6/71 (8.5)	$P = 0.498$
Negative ($n = 119$)	7/119 (5.9)	
Total ($n = 190$)		

cCR clinical complete response

* Chi-square test

Evaluation by ad-ERE–GFP assay of ER status in NAC

In our previous studies, we produced our own focused microarray for estrogen-regulated genes [16], and found that ER-positive breast cancers did not always show high expression of a target gene [unpublished data]. This suggests some discrepancy between the expression levels of ER protein and its function as a transcription factor. Using the ad-ERE–GFP assay system to detect ERα transcriptional activity in breast cancer cells, we analyzed the significance of ERα in the clinical response to NAC.

First, as shown in Fig. 1a and b, the relationship between response to paclitaxel and ERα expression was evaluated by IHC and the ad-ERE–GFP method, respectively, in 31 clinical samples. The cCR and cPR (clinical partial response) were sensitive to paclitaxel and the cSD (clinical stable disease) and cPD (clinical progressive disease) were insensitive. When ERα status was determined by IHC, 15 of 24 ER-positive cases (62.5%) and 4 of 7 ER-negative cases (57.1%) were paclitaxel-insensitive, while when ERα status was assessed based on its function by the ad-ERE–GFP method, 10 of 13 cases with high ER activity (76.9%) and 9 of 18 cases with low ER activity (50.0%) were paclitaxel-insensitive. These results suggest that the ad-ERE–GFP method might be more useful for the selection of ER-functional and paclitaxel-insensitive cases than the IHC method.

Next, we analyzed the response to paclitaxel in the 24 cases considered to be ERα-positive based on IHC (Fig. 1c). Seven cases showed pCR (pathological complete response) and 17 cases did not (non-pCR). Twelve cases of 24 cases showed low ER activity, indicating that ERα in these cases could not function as a transcription factor. The rate of non-pCR cases in the high ER activity group was 83.3% (10 of 12 cases), which was much higher than that in the low ER activity group, at 58.3% (7 of 12 cases). Consistent with the results on clinical response in NAC, the cases for which ERα did function as a transcription factor hardly achieve pCR. To further clarify the role of ERα in the sensitivity to paclitaxel, we carried out the following experiments in vitro.

Knockdown of ERα of MCF-7 cells increased the sensitivity to paclitaxel

On the basis of the clinical results, we analyzed whether or not ERα expression directly affects the sensitivity of breast cancer cells to paclitaxel. Figure 2a shows that siRNA-treated (si-1, si-2) MCF-7 cells were more sensitive to paclitaxel than the parent and scramble si-RNA cells. Figure 2b shows the ERα knockdown in si-1 and si-2 cells. While the IC50 values for the parent MCF-7 and scramble cells were 6.7 and 5.1 nM, those for si-1 cells and si-2 cells were 2.8 and 3.6 nM, respectively (Fig. 2c). These results suggest that ERα knockdown rendered MCF-7 cells more sensitive to paclitaxel than parent MCF-7 cells.
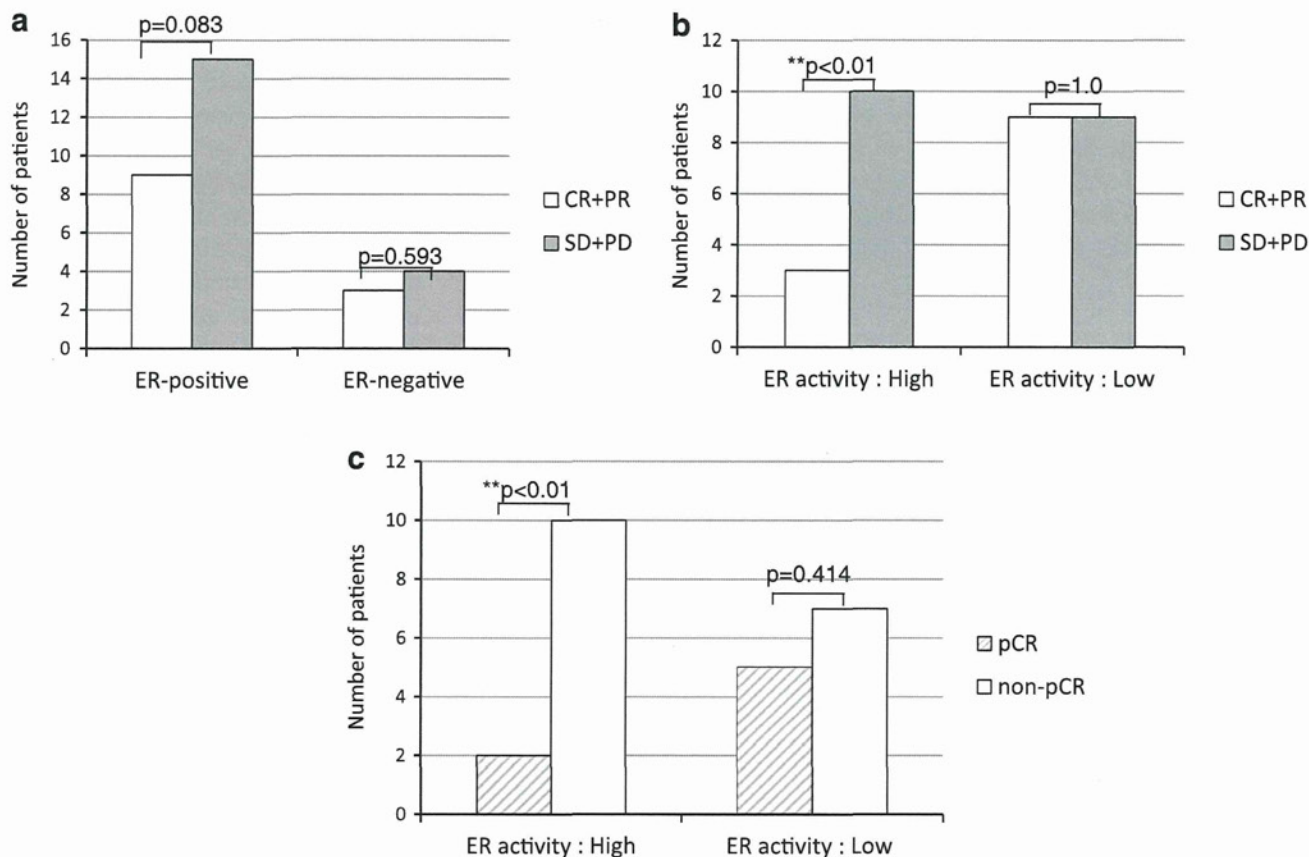
Fig. 1 The clinical evaluation and ER expression or activities in breast cancers in pre-NAC. **a** ERα status were evaluated by IHC method in 31 patients. **b** ERα activities were evaluated using adenovirus ERE–GFP system in 31 patients. **c** ER activities in pCR and non-pCR cases for 24 ER protein positive breast cancers

ERα expression decreased the sensitivity of ERα-negative SKBR3 cells to paclitaxel

Next, we examined the effect of ERα expression on the sensitivity of the SKBR3 cell line to paclitaxel. We generated SKBR3 cells expressing ERα, and compared the paclitaxel sensitivity of SK-ERpos cells with those of parent SKBR3 and SKBR3-vector control (SKBR3-cont) cells (Fig. 2d). Figure 2e shows ERα expression in SK-ERpos cells by real-time PCR. The IC50 values for the parent SKBR3 and SKBR3-cont cells were 3.6 and 3.1 nM, respectively, whereas that of SK-ERpos cells was >10 nM (Fig. 2f). These results suggest that ERα overexpression rendered SKBR3 cells more resistant to paclitaxel than parent SKBR3 cells.

SiRNA knockdown of ERα decreased deacetylation of α-tubulin

Paclitaxel promotes microtubule stabilization, which disrupts cellular processes, inhibits cell division, and ultimately induces apoptosis [23, 24]. On the other hand, estrogen promotes the deacetylation of tubulin through HDAC6, a downstream gene of ER, thereby increasing cell motilities via microtubule destabilization within the cells [18]. We examined the relationship between the presence of the ER and acetylation of α-tubulin.

Figure 3 shows results of the analysis for acetylation of α-tubulin in MCF-7 and ERα knockdown MCF-7 cells. We detected a significant increase in acetylated α-tubulin protein in ERα knockdown MCF-7 cells, suggesting that suppression of tubulin deacetylation by knockdown of ERα renders MCF-7 cells more sensitive to paclitaxel.

Upregulation of ERα function in paclitaxel-resistant MCF-7–E10 cells

To further evaluate the function of ERα in determining sensitivity to taxanes, we established paclitaxel-resistant MCF-7–E10 cells. MCF-7–E10 is an estrogen signal reporter cell line, which was derived from MCF-7 cell line via stable transfection of the ERE–GFP gene for the purpose of assessing ER activation [19, 20]. Paclitaxel-resistant MCF-7–E10 cells showed resistance to paclitaxel-

a

b

c

IC50 Values (nM)	
MCF7	6.66
Scramble	5.09
si-1	2.80
si-2	3.57

d

e

f

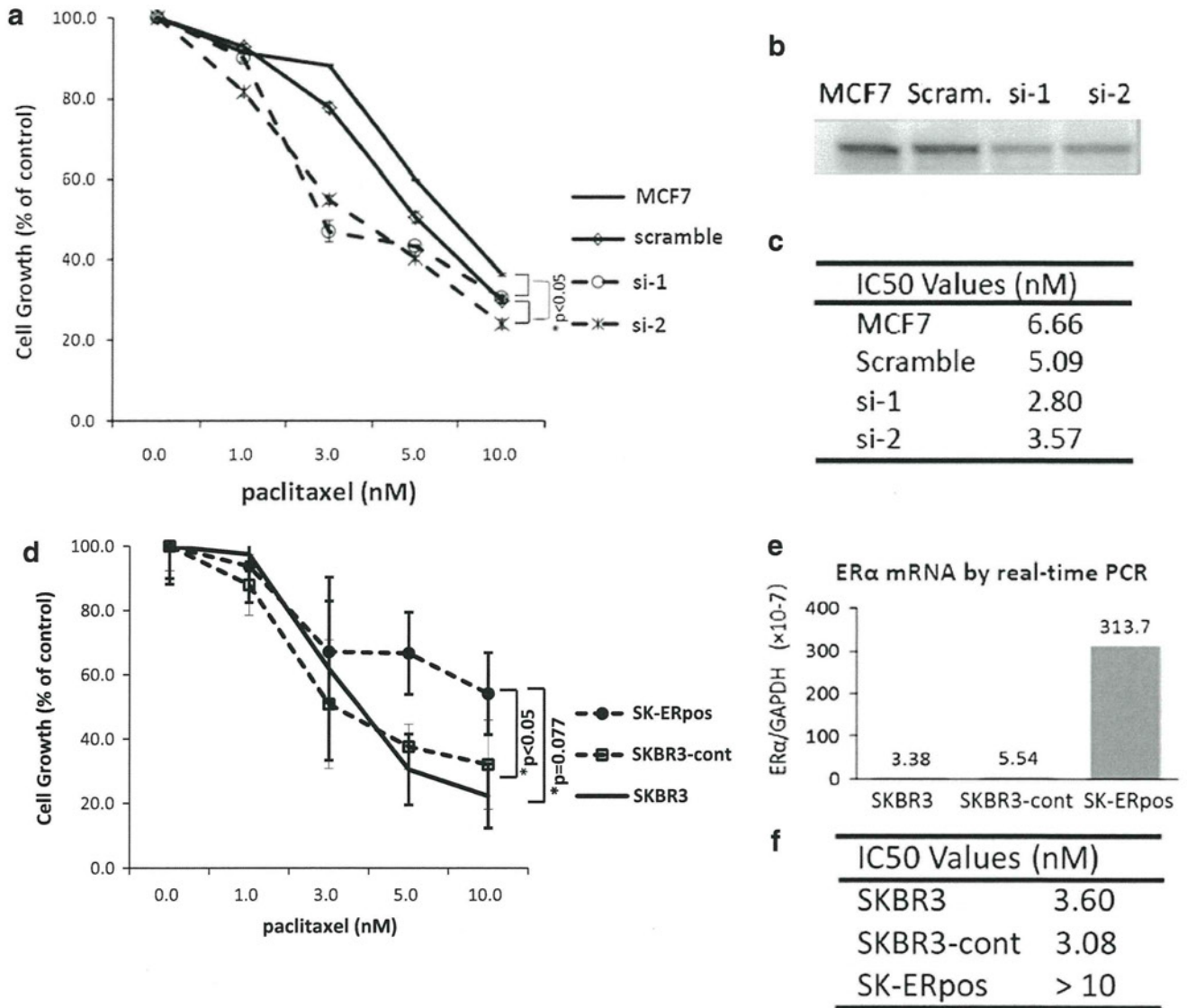| IC50 Values (nM)	
SKBR3	3.60
SKBR3-cont	3.08
SK-ERpos	> 10

Fig. 2 Knockdown of ERα in MCF-7 cells increased sensitivity to paclitaxel and over-expression of ERα decreased sensitivity to paclitaxel in SKBR3 cell lines. **a** Growth inhibition by paclitaxel in scramble and ERα siRNA-treated MCF-7 cells (si-1 and si-2), and parent MCF-7 cells. Cells were treated with paclitaxel at the indicated concentrations for 3 days in the normal culture medium supplemented with 10% FCS, which had not been deprived of estrogen, and the cell number was counted. The data shown as a percentage of the control are means ± SD of duplicate determinations of two independent experiments. *Bars* indicate SD. *$P < 0.05$ for ERα knockdown in MCF-7 versus parent and scramble MCF-7 by ANOVA. **b** Knockdown of ERα in MCF-7–si-1 and MCF-7–si-2 cells. ERα protein levels were assessed by western blotting. **c** IC50 values of paclitaxel in **a**. Knockdown of ERα rendered MCF-7 cells more sensitive to paclitaxel. **d** Growth inhibition by paclitaxel in parent, control, and ERα over-expressing SKBR3 cell lines. Cells were treated with paclitaxel at the indicated concentrations for 3 days and the cell number was then counted. The data shown as a percentage of the control are the means ± SD of duplicate determinations. *Bars* indicate SD. **e** ERα mRNA levels determined by real-time RT-PCR in parent, control, and ERα over-expressing SKBR3 cell lines. ERα mRNA levels were normalized relative to GAPDH. **f** IC50 values of paclitaxel shown in **d**

induced growth inhibition compared with parent MCF-7–E10 cells (Fig. 4a).

Next, we measured estrogen-dependent ERα activity via GFP expression using our automated system [22, 25]. ERα activities in paclitaxel-resistant MCF-7–E10 cells were measured after culture with estrogen for 3 days. Estrogen-dependent ERα activity in paclitaxel-resistant MCF-7–E10 clones was higher than that in parent MCF-7–E10 cells (Fig. 4b).

We examined the relationship between the presence of the ER and acetylation of HDAC6. Figure 4c shows ERα mRNA expression to be increased in paclitaxel-resistant
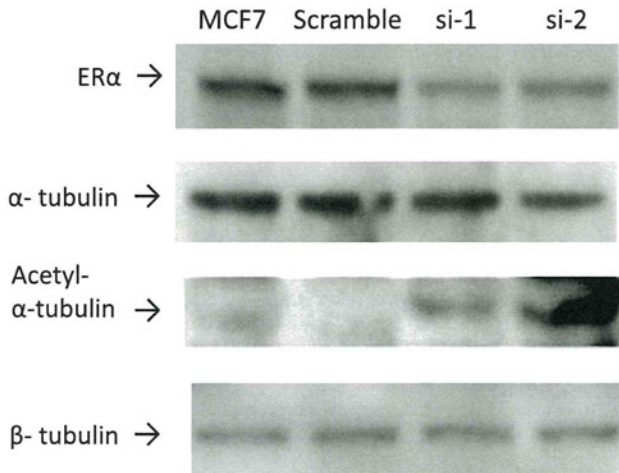
Fig. 3 SiRNA knockdown of ERα decreased deacetylation of α-tubulin. Western blotting of ERα, α-tubulin, and acetylated α-tubulin in scramble and ERα-siRNA-treated MCF-7 cells and parent cells. α-Tubulin was more acetylated in ERα-knockdown si-1 and si-2 MCF-7 cells

MCF-7–E10 cells. Figure 4d shows HDAC6 mRNA levels to be significantly increased in paclitaxel-resistant MCF-7–E10 cells. These results suggest that paclitaxel-resistant clones could be developed by increasing in HDAC6 expression via regulation of ERα expression.

Discussion

Patients with advanced breast cancer are at risk of tumor recurrence and death. Chemotherapy, especially NAC, has become the standard treatment for these patients to eradicate distant micrometastatic disease. In addition, NAC provides an ideal model for evaluating the role of biological markers such as the ER as prognostic factors. However, in the field of chemotherapy, there are few reports on predictive molecular markers for these patients. Therefore, we investigated the significance of ERα expression in the sensitivity of breast cancer to paclitaxel.

First, we compared clinical responses to taxanes in NAC between ER-positive and ER-negative cases. The results shown in Table 1 clearly demonstrate that ER-negative tumors are more sensitive to taxanes than ER-positive tumors. This result is consistent with previously reported observations for adjuvant chemotherapy.

Next, we analyzed the relationship between ERα expression and chemosensitivity to paclitaxel by comparing pCR, cCR, and cPR cases. We observed a discrepancy between the expression level of ER protein and ER transcription activity. This might be responsible for the difficulty choosing of the most appropriate chemotherapy. With the IHC method, 37.5 and 42.9% of ERα-positive and ERα-

negative breast cancers, respectively, were sensitive to paclitaxel (Fig. 1a). With the ERE–GFP method, 23.0 and 50.0% of high and low ER activity breast cancers, respectively, were sensitive to paclitaxel (Fig. 1b), suggesting that ERα-nonfunctional breast cancers are sensitive to paclitaxel. The ERE–GFP method differs significantly from the IHC method in the selection of ERα-nonfunctional cases.

Among 31 cases, we next analyzed 24 ERα positive breast cancers using the IHC method as shown in Fig. 1c. Twelve cases (50.0%) showed high ER activity when evaluated by the ad-ERE–GFP method. The cases with low ER activity showed a higher pCR rate (41.7%) than those with high ER activity (16.7%). Our results clearly show that, like ERα-negative breast cancer, the cases for which ERα protein could be detected but did not function as a transcription factor were liable to achieve pCR. Our result suggests that the ad-ERE–GFP method might more accurately predict the efficacy of chemotherapy than the IHC method, although studies with more samples are needed.

To examine the relationship between the presence versus absence of ERα expression and sensitivity to paclitaxel, we used two breast cancer cell lines, ERα-positive and HER2-negative MCF-7 cells and ERα-negative and HER2-positive SKBR3 cells. For each cell line, we analyzed the effects of altering in ERα expression levels on sensitivity to paclitaxel, and found that ERα expression directly affects the sensitivity to paclitaxel regardless of HER2 expression (Fig. 2a–f).

Finally, we analyzed the function of ERα in paclitaxel-resistant MCF-7 clones established in this study (Fig. 4a). Estrogen-dependent ERα activity in these PAC-resistant MCF-7 clones was higher than that in parent MCF-7 cells (Fig. 4b). Increased ERα expression is one mechanism whereby they showed high ERα activity (Fig. 4c), and expression of HDAC6 (Fig. 4d), identified as a target gene of the estrogen signal in our previous study [16], was also increased in these cells. These results that development of resistance to paclitaxel is associated with increased ERα expression and its activity in MCF-7 cells. We inferred from these observations that ER-positive breast cancer subjected to long-term treatment with paclitaxel chemotherapy becomes more sensitive to anti-estrogen drugs. We intend to study the interactions of paclitaxel and anti-estrogen drugs in treating ER-positive breast cancer further.

Taxanes act by shifting the dynamic equilibrium between tubulin and microtubules to the direction of microtubule assembly [23, 26]. Tubulin is the major component of microtubules, which play a critical role in cell migration, cell morphology, cell–cell interactions, and tumor interactions. Hubbert et al. reported that HDAC6 has been shown to deacetylate tubulin, target of taxane [18], and Palasso et al. suggested HDAC6 to be an important regulator of cell
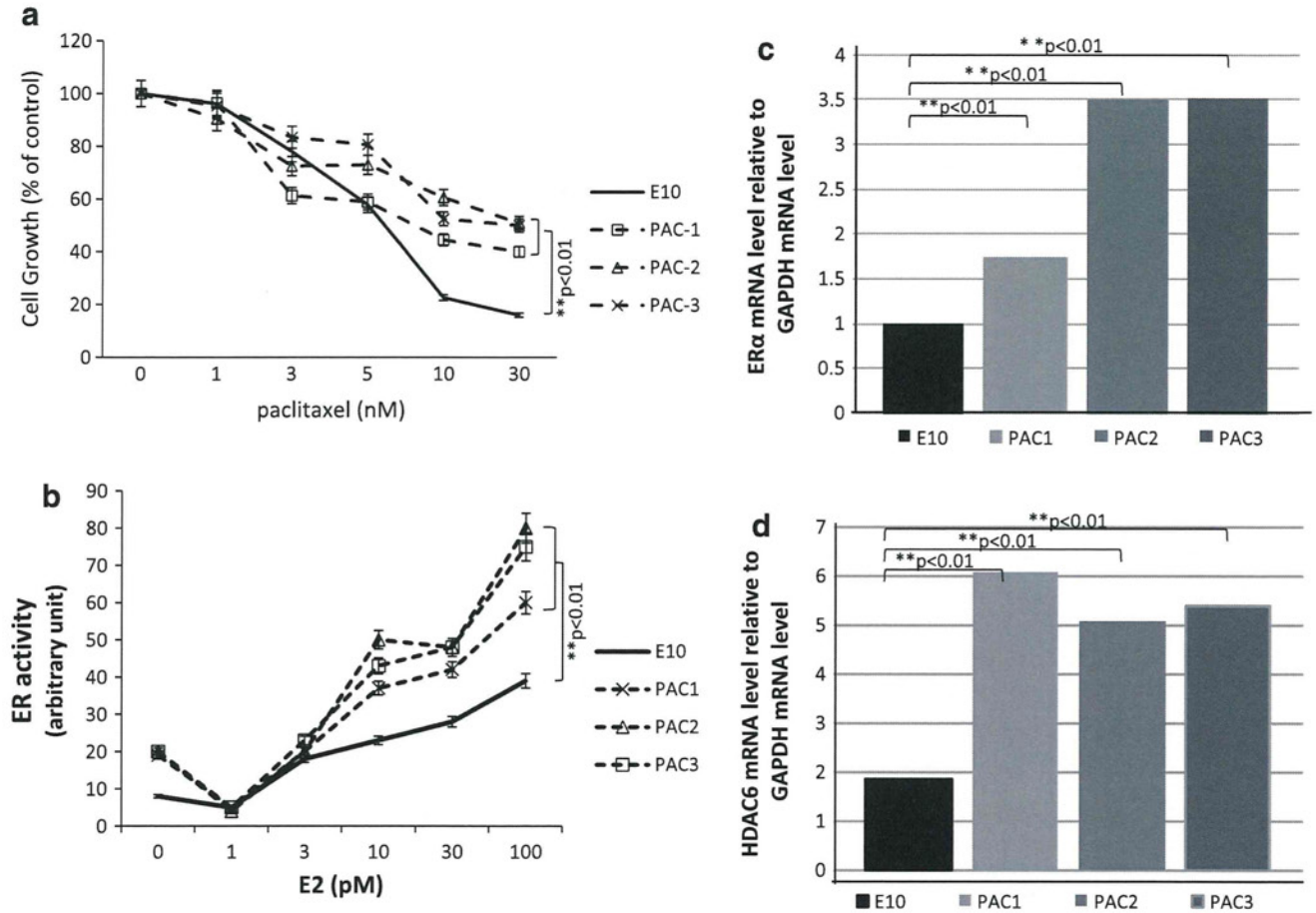
Fig. 4 Estrogen-dependent ER activities increased in paclitaxel-resistant MCF-7–E10 cells. **a** Resistance to paclitaxel-induced growth inhibition in PAC-1, PAC-2, and PAC-3–MCF-7–E10 cells. Cells were treated with paclitaxel at the indicated concentrations for 3 days and the cell number was then counted. The data are shown as a percentage of the means ± SD of duplicate determinations. *Bars* indicate SD. **b** Estrogen-dependent ER activities in PAC-1, PAC-2, and PAC-3–MCF-7–E10 cells. After 3 days of culture in estrogen-deficient medium, the cells were treated with estrogen at the indicated concentrations 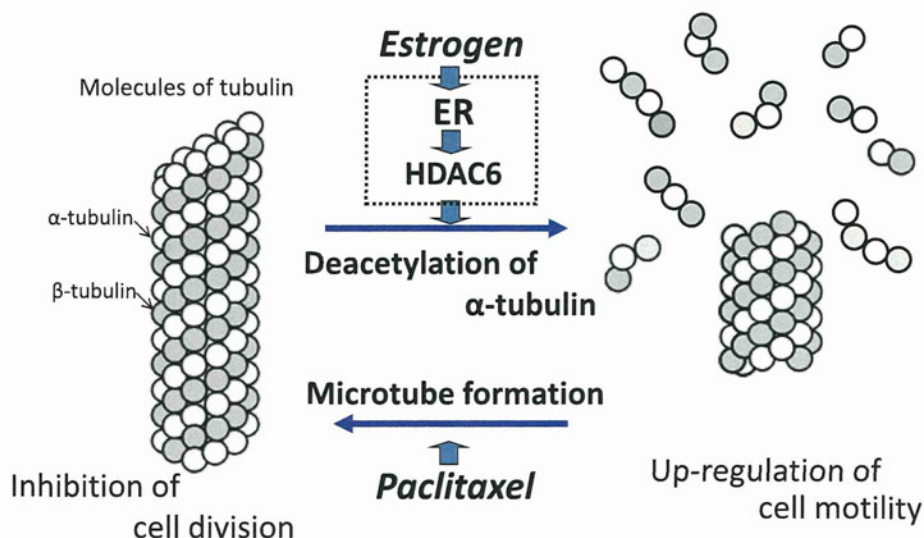for 3 days. ER activities were evaluated by expression of GFP using the automated image analysis system. $*P < 0.01$ for ERα activity in PAC-1, PAC-2, and PAC-3–MCF-7–E10 versus that in parent cells, by ANOVA. **c** ERα mRNA expression was increased in paclitaxel-resistant MCF-7–E10 cells (PAC-1, PAC-2, and PAC-3 cells). $*P < 0.01$ for ERα activity in PAC-1, PAC-2, and PAC-3–MCF-7–E10 versus that in parent cells, by ANOVA. **d** HDAC6 mRNA expression was increased in paclitaxel-resistant MCF-7–E10 cells (PAC-1, PAC-2, and PAC-3 cells). $*P < 0.01$ for ERα activity in PAC-1, PAC-2, and PAC-3–MCF-7–E10 versus that in parent cells, by ANOVA

motility, especially in ER-positive breast cancer [26]. In addition, in our previous study, HDAC6 overexpression caused tubulin deacetylation and enhanced the motility of breast cancer cells, while the inhibition of HDAC6 activity reduced motility [27]. Figure 3 shows α-tubulin to be more acetylated in ERα-knockdown MCF-7 cells and that ERα expression induced deacetylation of α-tubulin. The expression of HDAC6 was decreased in ERα-knockdown MCF-7 cells and increased in ERα-overexpressing SKBR3 cells (data not shown). HDAC6 and ERα mRNA expressions were also increased in paclitaxel-resistant MCF-7–E10 cells as described above. These results led us to hypothesize that ERα is involved in the regulation of tubulin, one of the targets of paclitaxel via HDAC6 expression.

Figure 5 is a schematic diagram showing how our findings in the present and previous studies are linked to the pharmacological properties of paclitaxel. In breast cancers having functional ERα, estrogen-induced HDAC6 expression caused tubulin deacetylation, which decreased the efficacy of paclitaxel via destabilization of tubulin. In other words, estrogen signals directly influence the effects of paclitaxel, which targets tubulin formation. Inhibition of HDAC6 might increase sensitivity to paclitaxel in ER-positive breast cancer, and we aim to establish more effective agents by developing HDAC6-targeting therapy.

This is the first report, to our knowledge, to provide evidence that ERα directly regulates tumor sensitivity to paclitaxel, primary via estrogen-induced deacetylation of

Fig. 5 Paclitaxel and estrogen show the opposite effects on tubulin assembly. Paclitaxel inhibits the proliferation of tumor cells via induction of microtubule formation, whereas estrogen induces deacetylation of α-tubulin via HDAC6. Our previous study has showed that deacetylation of α-tubulin causes up-regulation of cell motility [27]

Molecules of tubulin

Estrogen

ER

HDAC6

Deacetylation of α-tubulin

Microtube formation

Paclitaxel

α-tubulin

β-tubulin

Inhibition of cell division

Up-regulation of cell motility

tubulin involving HDAC6. These findings provide a new understanding of the mechanisms underlying the roles of the ER and chemotherapeutic agents such as paclitaxel, as well as insights into developing new molecular targets for breast cancer treatment.

References

1. Lippman ME, Allegra JC, Thompson EB et al (1978) The relation between estrogen receptors and response rate to cytotoxic chemotherapy in metastatic breast cancer. N Engl J Med 298:1223–1228

2. Conforti R, Boulet T, Tomasic G et al (2007) Breast cancer molecular subclassification and estrogen receptor expression to predict efficacy of adjuvant anthracyclines-based chemotherapy: a biomarker study from two randomized trials. Ann Oncol 18:1477–1483

3. Berry DA, Cirrincione C, Henderson IC et al (2006) Estrogen-receptor status and outcomes of modern chemotherapy for patients with node-positive breast cancer. JAMA 295:1658–1667

4. Green MC, Buzdar AU, Smith T et al (2005) Weekly paclitaxel improves pathologic complete remission in operable breast cancer when compared with paclitaxel once every 3 weeks. J Clin Oncol 23:5983–5992

5. Mazouni C, Kau SW, Frye D et al (2007) Inclusion of taxanes, particularly weekly paclitaxel, in preoperative chemotherapy improves pathologic complete response rate in estrogen receptor-positive breast cancers. Ann Oncol 18:874–880

6. Bear HD, Anderson S, Brown A et al (2003) The effect on tumor response of adding sequential preoperative docetaxel to preoperative doxorubicin and cyclophosphamide: preliminary results from National Surgical Adjuvant Breast and Bowel Project Protocol B-27. J Clin Oncol 21:4165–4174

7. Fisher B, Bryant J, Workmark N et al (1998) Effect of preoperative chemotherapy on the outcome of women with operable breast cancer. J Clin Oncol 16:2672–2685

8. Chollet P, Amat S, Cure H et al (2002) Prognostic significance of a complete pathological response after induction chemotherapy in operative breast cancer. Br J Cancer 86:1041–1046

9. Galdos C, Tarter PI, Estabrook A, Gistrak MA, Jaffer S, Bleiweiss IJ (2002) Relationship of clinical and pathologic response to Neoadjuvant chemotherapy and outcome of locally advanced breast cancer. J Surg Oncol 80:4–11

10. Chang JC, Wooten EC, Tsimelzon A et al (2003) Gene expression profiling for the prediction of therapeutic response to Docetaxel in patients with breast cancer. Lancet 362:362–369

11. Charles AG, Han TY, Liu YY, Hansen N, Giuliano AE, Cabot MC (2001) Taxol-induced ceramide generation and apotosis in human breast cancer cells. Cancer Chemother Pharmacol 47:444–450

12. Buzdar AU, Singletary SE, Theriault RL et al (1999) Prospective evaluation of paclitaxel versus combination chemotherapy with fluorouracil, doxorubicin, and cyclophosphamide as neoadjuvant therapy in patients with operable breast cancer. J Clin Oncol 17:3412–3417

13. Sledge GW, Neuberg D, Bernardo P et al (2003) Phase III trial of doxorubicin, paclitaxel, and the combination of doxorubicin and paclitaxel as front-line chemotherapy for metastatic breast cancer: an intergroup trial (E1193). J Clin Oncol 21:588–592

14. Martin M, Rodriguez-Lescure A, Ruiz A et al (2008) Randomaized phase 3 trial of fluorouracil, epirubicin, and cyclophosphamide alone or followed by paclitaxel for early breast cancer. J Natl Cancer Inst 100:805–814

15. Hayes DF, Thor AD, Dressler LG et al (2007) HER2 and response to paclitaxel in node-positive breast cancer. N Engl J Med 357:1496–1506

16. Inoue A, Yoshida N, Omoto Y et al (2002) Development of cDNA microarray for expression profiling of estrogen-responsive genes. J Mol Endocrinol 9:175–192
17. Zhang Z, Yamashita H, Toyama T et al (2004) HDAC6 expression is correlated with better survival in breast cancer. Clin Cancer Res 15:6962–6968
18. Hubbert C, Guardiola A, Shao R et al (2002) HDAC6 is a microtubule-associated deacetylase. Nature 417:455–458
19. Yamaguchi Y, Takei H, Suemasu K et al (2005) Tumor-stromal interaction through the estrogen-signaling pathway in human breast cancer. Cancer Res 65:4653–4662
20. Hayashi S, Niwa T, Yamaguchi Y (2009) Estrogen signaling pathway and its imaging in human breast cancer. Cancer Sci 100:1773–1778
21. Matsumoto M, Yamaguchi Y, Seino Y et al (2008) Estrogen signaling ability in human endometrial cancer through the cancer–stromal interaction. Endocr Relat Cancer 15:451–463
22. Yamaguchi Y, Hayashi S (2009) Estrogen-related cancer microenvironment of breast carcinoma. Endocr J 56:1–7
23. Pusztai L (2007) Markers predicting clinical benefit in breast cancer from microtubule-targeting agents. Ann Oncol 18(Suppl 12):15–20
24. Gan Y, Wientjes MG, Lu J, Au JL (1998) Cytostatic and apoptotic effects of paclitaxel in human breast tumors. Cancer Chemother Pharmacol 42:177–182
25. Hayashi S, Yamaguchi Y (2008) Estrogen signaling in cancer microenvironment and prediction of response to hormone therapy. J Steroid Biochem Mol Biol 109:201–206
26. Palazzo A, Ackerman B, Gundersen GG (2003) Cell biology: tubulin acetylation and cell motility. Nature 421:230
27. Saji S, Kawakami M, Hayashi S et al (2005) Significance of HDAC6 regulation via estrogen signaling for cell motility and prognosis in estrogen receptor-positive breast cancer. Oncogene 24:4531–4539

Antitumor activity of chemoendocrine therapy in premenopausal and postmenopausal models with human breast cancer xenografts

MOTOYUKI KATAOKA[1], YURI YAMAGUCHI[2], YOICHIRO MORIYA[1], NORIAKI SAWADA[1], HIDEYUKI YASUNO[1], KUMIKO KONDOH[1], DEAN B. EVANS[3], KAZUSHIGE MORI[1] and SHIN-ICHI HAYASHI[4]

[1]Product Research Department, Kamakura Research Laboratories, Chugai Pharmaceutical Co., Ltd., Kamakura 247-8530; [2]Research Institute for Clinical Oncology, Saitama Cancer Center, Saitama 362-0806, Japan; [3]Oncology Research, Novartis Institutes for BioMedical Research, Basel, Switzerland; [4]Center for Regulatory Epigenome and Diseases, Molecular and Functional Dynamics, Graduate School of Medicine, Tohoku University, Sendai 980-8575, Japan

Abstract. We examined the efficacy of chemoendocrine therapy using capecitabine as a chemotherapeutic agent in premenopausal and postmenopausal models with estrogen receptor (ER)-positive human breast cancer xenografts. Tamoxifen and letrozole were used as endocrine therapeutic agents for premenopausal and postmenopausal models, respectively. The antitumor activity of capecitabine in combination was significantly superior to either monotherapy treatment in both premenopausal ($p<0.01$) and postmenopausal ($p<0.05$) models. No increase in toxicity in terms of body weight loss was observed during treatment in either of the xenograft models. In the premenopausal model, the level of thymidine phosphorylase (TP), a key enzyme generating 5-FU from capecitabine, was upregulated ($p<0.05$) in tumors by tamoxifen but not by letrozole treatment in the postmenopausal model. The combination of 5'-deoxy-5-fluorouridine (5'-DFUR; an intermediate of capecitabine) with 4-hydroxytamoxifen (4-OHT; an active form of tamoxifen) or letrozole was also evaluated *in vitro* by using estrogen-responsive element (ERE) reporter gene assays aimed to model premenopausal and postmenopausal breast cancer. Both combinations decreased the number of estrogen-responding cells in a concentration-dependent manner and further analysis by isobolograms revealed a synergistic effect of the combination of 5'-DFUR with 4-OHT, and at least an additive effect of the combination of 5'-DFUR with letrozole. These results suggest that chemoendocrine therapy using capecitabine may be a useful treatment modality for patients with hormone-receptor-positive breast cancer, regardless of the menopausal status and should be explored in clinical trials.

Correspondence to: Dr Yoichiro Moriya, Product Research Department, Kamakura Research Laboratories, Chugai Pharmaceutical Co. Ltd., 200 Kajiwara, Kamakura 247-8530, Japan
E-mail: moriyayui@chugai-pharm.co.jp

Introduction

Two decades ago, *in vitro* antagonism in cytotoxicity was reported between chemotherapeutic agents and antiestrogens in breast cancer cells (1). This observation translated to the clinic as results with chemoendocrine therapies in patients have been disappointing (2,3). However, not all reports of addition of chemotherapies, such as CMF [a chemotherapy regimen consisting of cyclophosphamide, methotrexate and 5-fluorouracil (5-FU)], to endocrine therapies showed negative results. For example, clinical results from NSABP B-20 trial (4) and the International Breast Cancer Study Group (IBCSG) trial VII (5) indicated that the addition of CMF to tamoxifen yielded superior five-year disease-free survival rate. Therefore, it is likely that some chemotherapeutic agents may not be antagonistic to antiestrogens.

Capecitabine is an oral 5-FU derivative widely used for breast cancers which generates the active substance 5-FU in tumors by a three-step cascade of enzymes located in the liver and tumors. The final step is the conversion of 5'-DFUR, an intermediate metabolite, to 5-FU by TP, which is highly expressed in tumors. Therefore, a higher level of 5-FU would be expected in tumor tissues which have higher expression levels of TP, when treated with capecitabine. Indeed, it has been reported that the antitumor activity of capecitabine did correlate with tumor levels of TP activity in xenograft models, whereas that of 5-FU did not (6).

Estrogen is known to play a crucial role in estrogen receptor (ER)-positive breast cancer development and growth through binding to ER. It is reported that 71% of invasive breast cancer is ER-positive (7). Antiestrogen therapies are an indispensable treatment modality for almost all ER-positive breast cancer patients. Tamoxifen, an estrogen antagonist, was widely used for the treatment of ER-positive breast cancer patients with premenopausal, as well as postmenopausal, status. It was reported in a P-1 study that tamoxifen reduced the cumulative rate of invasive breast cancer (8), and that it reduced the incidence of contralateral breast cancer in premenopausal patients (9).

In postmenopausal women, the blood estrogen levels decrease because the ovaries cease to produce estrogen. However, estrogen level in breast cancer is still 10 times higher

than that in normal breast tissue (10,11) because estrogen is supplied through the conversion of androgen by aromatase, a key enzyme of estrogen synthesis. In addition, aromatase is known to be highly expressed in the adipose stromal cells adjacent to breast cancer cells (12). Thus, the locally produced estrogen promotes the growth of ER-positive tumor cells in postmenopausal breast cancer patients. Letrozole, an aromatase inhibitor, improved disease-free survival and time to distant recurrence compared to tamoxifen in postmenopausal ER-positive breast cancer patients (BIG 1-98 study) (13,14).

In the present study, we examined the antitumor activity of capecitabine in combination with endocrine therapies in both premenopausal and postmenopausal breast cancer xenograft models. We also examined the effect of the combination capecitabine plus antiestrogens in *in vitro* ERE reporter gene assays (15,16).

Materials and methods

Chemicals. Capecitabine and 5'-DFUR were synthesized at Hoffmann-La Roche (Basel, Switzerland). Tamoxifen citrate, 4-hydroxytamoxifen (4-OHT) and androstenedione were purchased from Sigma-Aldrich Co. (St. Louis, MO). Letrozole was obtained from Novartis Pharmaceutical Co., Ltd.

For *in vivo* study, capecitabine was dissolved in 40 mmol/l citrate buffer, pH 6.0 containing 5% gum arabic. Tamoxifen was dissolved in the same buffer as capecitabine solution. Letrozole was dissolved in dimethyl sulfoxide, and further diluted with 0.5% aqueous solution of sodium carboxymethylcellulose containing 20% propylene glycol. For *in vitro* study, 5'-DFUR was dissolved in phosphate-buffered saline (10 mmol/l). 4-OHT was dissolved in ethanol (1 mmol/l), and further diluted with phosphate-buffered saline, pH 7.4. Letrozole was dissolved in the same manner as in the *in vivo* study.

Animals. Female 4-5-week-old BALB/c-nu/nu mice [CAnN. Cg-Foxn1(nu)/CrlCrlj nu/nu] were obtained from Charles River Laboratories Japan, Inc. (Yokohama, Japan). All mice were housed in a pathogen-free environment under controlled conditions (temperature 20-26°C, humidity 40-70%, light/dark cycle 12 h/12 h). Chlorinated water and irradiated food (CE-2; Clea Japan, Inc., Tokyo, Japan) were provided *ad libitum*. All mice were allowed to acclimatize and recover from shipping-related stress for at least 1 week prior to the study. The health of the mice was monitored by daily observation. The protocol was reviewed by the Institutional Animal Care and Use Committee of Chugai Pharmaceutical Co., Ltd. and all mouse experiments were performed in accordance with the Guidelines for the Accommodation and Care of Laboratory Animals promulgated in Chugai Pharmaceutical Co., Ltd.

Cell lines and culture conditions. Estrogen receptor-positive MCF-7 human breast cancer cell line was kindly provided by Dr Y. Iino (Gunma University, Maebashi, Japan) and was maintained in Eagle's minimum essential medium (MEM; Sigma-Aldrich Co.) supplemented with 0.1 mmol/l MEM non-essential amino acids (Invitrogen Corp., Carlsbad, CA), 1 mmol/l sodium pyruvate (Invitrogen Corp.) and 10% (v/v) heat-inactivated fetal bovine serum (FBS; Thermo Trace Ltd., Victoria, Australia).

Preparation of aromatase transfectant. The aromatase gene transfectant cell line MCF-7A25F3 was established according to the method of Zhou *et al* (17). Briefly, the first-strand cDNA synthesis was carried out with 5 µg of total RNA from human placenta (Toyobo Co., Ltd., Osaka, Japan), 100 pmoles of oligo (dT) and 200 units of SuperScript II (Invitrogen Corp.). The target cDNA for aromatase gene was obtained by the polymerase chain reaction. The sequences of the primer were as follows: forward; 5'-GCT CTA GAG GAA CAC AAG ATG GTT TTG GAA-3' containing *Xba*I restriction site for cloning, reverse; 5'-GCT CTA GAT GGG TAC TGA CCA GCC TTC T-3'. The PCR product was digested with *Xba*I and then was extracted from the gel. The cDNA fragment was inserted into the *Xba*I and *Sma*I site of the mammalian expression vector pCI-Neo (Promega Co., Ltd., WI). The plasmid DNA was purified using DNA miniprep column (Qiagen GmbH, Hilden, Germany) according to the manufacturer's instruction and then sequenced.

This sequence-confirmed construct was used for the transfection to generate the MCF-7 cell line expressing aromatase gene. To establish a stably transfected cell line, 1 µg of plasmid DNA was incubated with 0.5 ml of Lipofectamine (Clontech Laboratories Inc., CA) for 30 min and overlaid onto 1x10⁶ MCF-7 cells for 1 h in serum-free medium. Cells were then selected in the presence of 350 µg/ml Geneticin (G-418; Calbiochem Co., Ltd., San Diego, CA). After selection for 2 weeks, the cells were screened for aromatase cDNA in genomic DNA by PCR. The ratio of copy numbers of aromatase cDNA in the parent MCF-7 cells and in the transfected cells were estimated. Primers for quantification were as follows: forward; 5'-GGA AAT GCT GAA CCC GAT AC-3', reverse; 5'-GAG AAA AAG GCC AGT GAG GA-3' for aromatase, and forward; 5'-GGT TGG CCA ATC TAC TCC CAG G-3', reverse; 5'-TGG TCT CCT TAA ACC TGT CTT G-3' for β-globin. The copy number of the aromatase gene of the transfected cells as a whole was 2-fold higher than that of the parent MCF-7 cells. The cloning of transfected cells was performed and clones revealing a high proliferation response to androstenedione were selected. Next, the clones were inoculated into ovariectomized BALB/c-nu/nu mice which had been implanted with a slow-release androstenedione pellet to determine the tumor growth in response to the hormone *in vivo*.

Measurement of aromatase activity. Aromatase activity was determined by using a tritiated water (^{3}H$_2$O) method in which the ^{3}H$_2$O released from 1β-^{3}H-androstenedione was measured. The measurement was conducted by Teikoku Hormone Medical Co., Ltd. (Kawasaki, Japan). Briefly, the collected MCF-7A25F3 cells were homogenized and centrifuged at 200 x g for 3 min. The supernatant (0.5 ml) was incubated with 1β-^{3}H-androstenedione and NADPH at 37°C for 60 min. The incubation was terminated by cooling, and the reaction mixture was extracted with 2 ml of ice-chilled chloroform. The aqueous layer was removed and mixed with 100 mg of activated charcoal. The mixture was vortexed well and centrifuged at 1,500 x g for 10 min at 4°C to remove the charcoal. An aliquot (0.5 ml) of the supernatant was added to 8 ml of Scintisol fluid (Dojin Chemical Co., Kumamoto, Japan) in scintillation vials, vortexed, and measured for radioactivity. Blank values were subtracted, and the aromatase activity was expressed as fmol